Simple Topographic Parameter for Along-trench Friction Distribution of Shallow Megathrust Fault

Hiroaki Koge[1], Juichiro Ashi[2], Jin-Oh Park[3], and Ayumu Miyakawa[4]

[1]National Institute of Advanced Industrial Science and Technology, AIST
[2]University of Tokyo
[3]Atmosphere and Ocean Research Institute, University of Tokyo
[4]National Institute of Advanced Industrial Science and Technology

November 26, 2022

Abstract

In the 2011 Tohoku-Oki earthquake, the rupture in the subduction megathrust reached the trench axis and triggered a large tsunami. The shallow portion of the subduction megathrust fault was regarded as an aseismic stable zone. The frictional properties along the shallow subduction plate boundary are an important foundation for understanding the cause of the dynamic fault rupture in the earthquake near the trench. The critical taper model of a sedimentary wedge best describes the first-order mechanics of a subduction zone wedge. The tapered wedge geometry (slope angle α and basal dip angle β) is responsible for the strength of a shallow megathrust. However, to apply the critical taper model for the investigation of spatial heterogeneity, we need to improve handling β, since β is derived from the subsurface structure and its value depends on the number of accurately depth-converted seismic profiles. Here, the effect of décollement dip angle β in the critical taper model of a sedimentary wedge is examined. The effect is negligible for a high pore fluid pressure ratio, allowing the frictional variation to be obtained with only bathymetry data. We applied the model to the Japan Trench. The frictional variation indicates that a smaller frictional area corresponds to an area with a larger coseismic shallow rupture during the 2011 earthquake than those of the southern and northern areas. The method can be applied to other trenches to predict seismic potential.

Hosted file

`kogeetal2020_agusupporting.docx` available at https://authorea.com/users/535290/articles/606478-simple-topographic-parameter-for-along-trench-friction-distribution-of-shallow-megathrust-fault

Simple Topographic Parameter for Along-trench Friction Distribution of Shallow Megathrust Fault

H. Koge[1*], J. Ashi[2,3], J.-O. Park[2], A. Miyakawa[1]

[1] Geological Survey of Japan, National Institute of Advanced Industrial Science and Technology, Central 7, 1-1-1 Higashi, Tsukuba, Ibaraki 305-8567, Japan

[2] Atmosphere and Ocean Research Institute, The University of Tokyo, 5-1-5 Kashiwanoha, Kashiwa-shi, Chiba 277-8564, Japan

[3] Department of Natural Environmental Studies, Graduate School of Frontier Sciences, The University of Tokyo, 5-1-5 Kashiwanoha, Kashiwa-shi, Chiba 277-8564, Japan

*Corresponding author: Hiroaki Koge (koge.h@aist.go.jp)

Key Points:

- In high pore fluid pressure, the along-trench friction distribution of megathrust is allowed to be obtained with only bathymetry.
- The frictional distribution of the Japan Trench corresponds to an area with large-coseismic rupture in the 2011 earthquake.
- The method can be applied to other subduction zones to predict seismic potential.

Abstract

In the 2011 Tohoku-Oki earthquake, the rupture in the subduction megathrust reached the trench axis and triggered a large tsunami. The shallow portion of the subduction megathrust fault was regarded as an aseismic stable zone. The frictional properties along the shallow subduction plate boundary are an important foundation for understanding the cause of the dynamic fault rupture in the earthquake near the trench. The critical taper model of a sedimentary wedge best describes the first-order mechanics of a subduction zone wedge. The tapered wedge geometry (slope angle α and basal dip angle β) is responsible for the strength of a shallow megathrust. However, to apply the critical taper model for the investigation of spatial heterogeneity, we need to improve handling β, since β is derived from the subsurface structure and its value depends on the number of accurately depth-converted seismic profiles. Here, the effect of décollement dip angle β in the critical taper model of a sedimentary wedge is examined. The effect is negligible for a high pore fluid pressure ratio, allowing the frictional variation to be obtained with only bathymetry. We applied the model to the Japan Trench. The frictional variation indicates that a smaller frictional area corresponds to an area with a larger coseismic shallow rupture during the 2011 earthquake than those of the southern and northern areas. The method can be applied to other trenches to predict seismic potential.

Plain Language Summary

We improve a method for obtaining along-trench basal friction with high spatial resolution and the results of the application correlates with the earthquake rupture.

1 Introduction

The study of shallow megathrust faults has become the focus of research on large disaster mitigation. Conventionally, the shallowest portion of a subduction megathrust fault (i.e., décollement) is expected to resist earthquake rupture and is considered to be an aseismic stable zone with low-level locking, as opposed to the deeper seismogenic zone with strong locking (e.g., Bilek & Lay, 2002; Currie et al., 2002). However, in the 2011 Tohoku-Oki earthquake (Mw 9.0), the coseismic rupture and slip propagated to the shallow portion of the subduction zone. According to observations, the surface of the trench landward slope moved tens of meters, suddenly disturbing the seawater, and eventually generating a devastating tsunami (Fujiwara et al., 2001; Kodaira et al., 2012; Sun et al., 2017). This 2011 event has thus changed our understanding of tsunami generation and rupture mechanics in such shallow zones. Core samples and continuous geophysical logging from scientific drilling (IODP Exp. 343/343T) for the shallow megathrust in the Japan Trench indicate that an important reason for the large slip is that the shallow fault zone is thin and weak (Chester et al., 2013; Fulton et al., 2013; Ujiie et al., 2013).

However, it is unknown whether the large slip in the shallow portion is representative of the Japan Trench or reflects site-specific geological conditions. The mechanical conditions of the plate boundary fault are the key to answering this question. The critical taper model best describes the first-order mechanics of a subduction zone wedge (e.g., Dahlen, 1990; Wang et al., 2019; Wang & Hu, 2006) and can be used to estimate the strength of a shallow megathrust fault (Fig. 1). This mechanical model is based on the Mohr-Coulomb failure criteria. It states that the tapered wedge geometry (slope angle α and basal dip angle β) is determined by the relative strengths of the wedge materials and the effective friction of the megathrust fault (μ_b') (Wang & Hu, 2006). Previous studies have used the critical taper model to estimate the along-trench friction distribution of a megathrust fault with seismic reflection profiles, obtaining information about mechanisms related to seismic activity (Fagereng, 2011; Koge et al., 2014). However, there is the problem to discuss the spatial heterogeneity of the frictional variation with the seismic activity. The spatial resolution of the frictional distribution is insufficient for comparison with previous research, because the number of profiles that can be used for the critical taper model is insufficient. For example, the distribution was based on only 3 or 12 transects in previous studies (Fagereng, 2011; Koge et al., 2014).

Cross sections are required for handling the basal dip angle β. The parameter β is derived from the subsurface structure and its value depends on the number of accurately depth-converted seismic profiles. The reliability of comparison for μ_b' is insufficient if β is not estimated with the seismic profiles converted by the same velocity model (details given below).

Therefore, to determine the along-trench frictional heterogeneity of a shallow megathrust fault with high-density and high-precision friction, we must first improve the handling of β. In this study, we theoretically verify the effect of β in the calculation of μ_b'. Then, we apply the critical taper model to the Japan Trench. The results show that the effect of β can theoretically be ignored when a high pore pressure ratio is used. We can thus obtain the μ_b' distribution using only bathymetrya.

2 Revisit of Coulomb wedge and critical taper theory

We review the Coulomb wedge and critical taper theory to highlight the difficulty of using the basal dip angle (β) and to demonstrate the workaround for a natural accretionary wedge. Critical taper theory, first introduced by Davis et al. (1983) and Dahlen (1984), is a mechanical model based on Mohr-Coulomb criterion. It summarizes how the wedge geometry (surface slope angle α and basal dip β) is controlled by wedge strength and basal μ_b'. The theory has been applied to subduction zones in various studies to describe the first-order mechanics, namely the physical properties and deformation of wedges (e.g., Wang et al., 2010, 2019; Wang & Hu, 2006). By assuming that (i) the tip of the wedge is tapered, (ii) the sediments added to the prism are non-viscous, and (iii) the internal stress is always at the critical state just before failure, the taper angle α + β of the wedge is controlled by the relative strengths of the wedge materials and basal fault, i.e., the coefficient of internal friction averaged over the wedge μ, the pore fluid pressure ratio within the wedge λ, and the effective coefficient of basal friction μ_b'. However, β is difficult to obtain except for the seismic profile. Here, we demonstrate that β can be ignored in the calculation of friction for a natural accretionary wedge.

2.1 Effective coefficient of basal friction for critical taper theory

In the critical taper model, we obtained the effective coefficient of basal friction and pore fluid pressure ratio by drawing cross plots between λ and μ_b' (Wang and Hu, 2006; Wang et al., 2010, Wang et al., 2019) (Fig. 2A). Here, we describe how to simply obtain the effective coefficient of basal friction from seismic profiles.

First, the modified slope angle α in the subaerial condition is formulated as

$$\alpha^{\prime} = tan^{-1}\left[\left(\frac{1-\rho_w/\rho}{1-\lambda}\right)tan\alpha\right]$$

where α is a parameter available from the profile, ρ is the wedge sediment density, ρ_w is the fluid density, and λ is the pore fluid pressure ratio. Then, the uniform angle between the most compressive principal stress σ_1 and the upper surface ψ_0 is formulated as

$$\psi_0 = \frac{1}{2} sin^{-1}\left(\frac{sin\alpha'}{sin\phi}\right) - \frac{1}{2}\alpha'$$

where φ is the angle of internal friction within the wedge. ψ_0 is the angle between σ_1 and the upper slope. Under the non-cohesive condition, this equation is valid in the entire wedge except at the boundary and the basement. In the Mohr-Coulomb criterion, $\tau = \sigma \cdot tan\phi + C$, where τ is the shear stress, σ is the vertical stress, $tan\phi$ is the internal friction coefficient (also written as μ), and C is the cohesion force, the cohesion can be neglected when dealing with huge geological structures. This equation implies that the shear stress to failure is described by internal friction and cohesion forces, the internal friction forces are proportional to the vertical stress, and the cohesion forces are independent of the vertical stress. For large geological structures, therefore, C is small enough to be negligible because of the large order of σ. Because along-strike stresses are not regarded in the critical taper model, the following simple geometric formula of the critical taper model can be applied:

$$\alpha + \beta = \psi_b - \psi_0$$

where ψ_b is the angle between σ_1 and the basal surface. Then, the effective coefficient of basal friction (μ_b') is obtained from the Mohr-Coulomb criterion and the stress balance of the basal condition as

$$\mu_b' = \frac{tan2\psi_b}{csc\phi sec2\psi_b - 1}$$

To draw the limb of the cross plot between μ_b' and λ, we set λ in the range between 0 and 1 (Fig. 2A). All extensionally critical states form the left limb of the critical state curve and all compressively critical states form the right limb. A stable field coincides with the critical state curve. The red straight line that intersects the critical state curve ideal the assumed the pore fluid pressure ratio λ. By assuming λ to be a constant parameter, we can obtain μ_b' from the intersection of λ and the limb curves calculated earlier.

Here, for example, we assume the following conventional wedge parameters: ρ = 2700 k/m^3, ρ_w = 1000 kg/m^3, and λ = 0.88 (Lallemand et al., 1994) in Fig. 2A. μ_b' can be calculated from the intersection of λ = 0.88 and the curves (Wang et al., 2019). Because the wedge should be in a constant compressively critical state just before failure, we focus on only the intersection with the right limb. Thus, we can obtain μ_b'= 0.06.

2.2 Difficulty in handling β

α can be obtained from not only the seismic profiles but also bathymetry, which are widely accessible. In contrast, β is a parameter of the underground geometry and thus the seismic profile is necessary. The number of seismic cross sections is relatively small in the subduction zone. For example, in previous research (Fagereng, 2011; Koge et al., 2014), for friction variation, there were insufficient profiles to calculate the effective coefficient of basal friction at the plate boundary to compare seismic activity. Furthermore, even if there are enough seismic profiles, there are other problems. The depth accuracy when obtaining β has not been sufficiently discussed (Fig. 1A). Because the depth of a plate boundary fault depends on the velocity model of the seismic analysis, it greatly affects the value of β. For a comparison of each subduction or transect, if the target is on the scale of several kilometers, the reflection seismic profile with pre-stack depth migration is practical for high precision. If the target is on a wider scale, it is desirable to use the reflection profile converted to the depth model with the velocity structure from the refraction. Thus, the number of seismic profiles that can be used for the critical taper model is more limited. Therefore, to obtain the along-trench friction distribution of the shallow megathrust fault with higher density and precision friction, we first need to improve the handling of β in the critical taper model.

The change of the shape of the wedge reflecting the dynamic state of stress within the wedge can be a problem during the seismic cycle (Wang and Hu, 2006). But the magnitude of the change of geometry including α and β is so minor that our calculation based on the static Coulomb wedge is not affected. For example, a comparison of the topography before and after the earthquakes shows the 50-m extension of the tip portion of the wedge (Fujiwara et al., 2011). However, since, the whole wedge shape is larger body than the meter-scale that it should be assumed almost the same as before and after the 2011 earthquakes.

2.3 Slight effect of β on calculation of μ_b'

We found the blind spot of the critical taper theory that β does not significantly influence the calculation of the friction when a high pore fluid pressure ratio is used. We graphed the fluid pressure ratio within the prism (λ) versus effective basal friction (μ_b'); the straight and broken lines represent different states of β (Fig. 2B). Here, we assume the parameters to be the representative values in the conventional subduction zones, as above (Lallemand et al., 1994). In Fig. 2B, the change of β (from 1° to 5°) dominates the change in the width of the curve. However, with a high λ, the intersection is near the curve peak. Therefore, the change in the width due to a change in β has an only slight effect on the change in μ_b'. The β range of 1° to 5° covers most of the subduction zone (Lallemand et al., 1994). This small effect of β should be regarded in the general subduction zone, especially for a high λ.

To determine the actual effect of β, we calculated μ_b' with α and β varied from 1° to 5° and applied multiple regression analysis to the result. In the calculation, we assumed the following representative values in the conventional subduction zones (Lallemand et al., 1994): pore fluid pressure ratio λ = 0.88, internal friction angle φ = 34°, and wedge density ρ = 2700 k/m^3. (Table S1, Fig. 2C). The taper angle α + β should be much less than 10° (Wang et al., 2006). Because the calculation cannot be conducted when α = β = 0, the results obtained under this condition**.** were removed. In the graph, the difference in inclination shows the influence. In the results of multiple regression analysis, the influence of α was 76.8% and that of β was 23.2%. Because the shallow subduction portion (the target for the Japan Trench) should be in an initial stage of consolidation in the compressive state with subduction, it can be considered that high λ is valid and that φ is smaller than the assumed value. For example, Wang et al. (2019) targeted almost the same portion of the Japan Trench and assumed λ = 0.8 and φ = 21.8°. In this case, the actual effect of α was 79.7% and that of β was 20.3%. They assumed λ = 0.8 to indicate a weak crust. However, when applied to the Japan Trench, a higher λ can be assumed; Kimura et al. (2012) found λ > 0.95.

Therefore, the slope angle of the seafloor well represents the friction coefficient in a high-pore-fluid-pressure environment because β has little effect on μ_b' in the general subduction zone. It is necessary to evaluate the effect of β at certain subduction zones, especially based on λ and φ (like in Table S1 and Fig. 2C), and determine whether this assumption is valid.

3 Application of bathymetric critical taper model to Japan Trench

3.1 Slope angles along Japan Trench

As mentioned above, we can assume the landward slope angle α indicates the effective basal friction (μ_b'). In other words, by obtaining the distribution of α along the trench, it is possible to obtain the relative frictional distribution. In the case of the Japan Trench, the influence of α is 79.7% (λ = 0.8, φ = 21.8°).

To obtain an accurate α distribution in the Japan Trench, we first obtained α from only the lower slope in the Japan Trench to avoid the influence of the slope break (i.e., the change point of the slope angle). In the Japan Trench, the slope in the profile can be separated into three sections, namely higher slope, middle slope, and lower slope (Tsuru et al., 2002), defined by slope breaks. If we set the angle of the slope across the slope break, accuracy will decrease. The lower slope of the Japan Trench is defined as a distance of approximately 25 km horizontally from the trench axis. Furthermore, we developed a straight-line approximation formula for the lower slope, and then adopted the approximation (R > 0.9) for α (Table S2).

Although it is preferable to take the bathymetric profile for α in the direction of maximum inclination, if the deviation from the direction is about 18°, the error can be kept within 5%. This is explained geometrically below.

The slope (OM) acquired when the maximum inclination direction (OL) is unintentionally off by θ is defined as α_m (Fig. 3A). The slope angle α_m is obtained from the acquired slope (OM). This OM is assumed to deviate from the maximum inclination direction (OL) by θ (Fig. 3B). In this situation, α_m is $tan^{-1}(MM'/OM')$ in triangle OMM' (Fig. 3B). OB is shown in Fig. 3A; OM = R. For MM', we need to consider the other triangle in Fig. 3C. NN' in Fig. 3C is the same as MM' in Fig. 3B. Because NN' is $Rtan\alpha - R(1-cos\theta)tan\alpha = Rcos\theta \cdot tan\alpha$ in Fig. 3C, we obtain MM' as NN' = $Rcos\theta \cdot tan\alpha$. From this, the slope angle α_m shifted by θ from the maximum inclination direction is $tan^{-1}(B\,B'/OB)tan^{-1}(cos\theta \cdot tan\alpha)$. The ratio α_m/α is calculated with θ from 0° to 45° (α = 10°; the maximum slope angle in this research does not exceed this). If $\theta \leq 18°$, the ratio α_m/α is within 95%. Because θ is drawn as 18° in Fig. 3A, it can be understood that if the deviation is like that in this figure, we do not have to care the difference of θ.

3.2 Friction distribution of shallow megathrust fault in Japan Trench

To consider whether the huge tsunami was triggered due to site-specific geological conditions, we applied the approximation method of the critical taper model to the Japan Trench and obtained the friction coefficient distribution of the shallow plate boundary fault. Using the compiled 250-m grid (Kishimoto, 2000) at the horizontal 25 km focused on the shallow portion, we obtained the distribution of α as the relative friction distribution of the shallow megathrust (Fig. 4).

We found that the low-α segment at approximately 36° - 39° N corresponds to the coseismic slip distribution for the 2011 Tohoku-Oki earthquake (Chester et al., 2013). Based on this, the earthquake that occurred in the low-α segment could have overshot, making the slip propagate to the shallow portion of the plate boundary fault due to the low friction of the shallow portion, leading to the huge tsunami. On the south and north ends of the distribution, there are relatively high-friction areas. Thus, the slip could not propagate to the other segments (the high friction acted as a barrier). In other words, the low friction in the shallow area is considered to have caused the huge tsunami. In addition, the low-α segment in this study mostly corresponds to the location of the central segment along the Japan Trench indicated by the distribution of seismic activity with the S-net ocean-bottom seismograph network (Nishikawa et al., 2019). The Japan Trench margin might be generally under a low friction condition, except for regions where the high friction condition caused by just subducted the seamount (Mochizuki et al., 2008) or the petit-spot volcanoes (Hirano et al., 2006) dominant. Because λ and φ are parameters stored in μ_b', it is not possible to determine whether the variation in α (i.e., relative μ_b') is due to a change in physical properties or a change in pore water pressure. Although we could not separate the effect of the physical properties and the pore pressure on α, both effects reflect the strength of the megathrust, confirming our assertion.

4 Conclusions; approximation of distribution of landward slope angle from friction coefficient distribution of megathrust fault

The proposed approach can be used to better characterize basal friction along the shallow megathrust in other margins. Correlations between the frontal prism surface slope and the extent of the 2011 Tohoku rupture patch were observed.

We reviewed the formulas in the critical taper model used for calculating the effective coefficient of basal friction and found that the effect of β on basal friction can be regarded as slight in the general subduction zone, especially under high-fluid-pressure-ratio (λ) conditions. In other words, the along-trench friction variation of a shallow megathrust can be determined based on only the α distribution. The basal friction is conventionally obtained by drawing the curves of the fluid pressure ratio within the prism (λ) versus effective basal friction (μ_b') in the subduction zones. The coefficient of friction is obtained from the intersection of the curve and the red straight line (fixed λ). However, with a high λ (most wedges), this intersection is near the curve peak (Fig. 2B). Therefore, the change in width caused by the change in β has only a slight effect on μ_b'. The trench landward slope angle α (i.e., relative μ_b') can then be easily obtained using existing global bathymetry data (such as ETOPO1) or observed bathymetry; therefore, the friction distribution can be easily obtained with higher density and precision. This idea is quite similar or contrapositive to the newly proposed that megathrust shear force controls mountain height at convergent margin (Dielforder et al., 2020). But, Dielforder et al. (2020) have proposed the method to estimate the megathrust shear force in subduction zones from the rheological approach, which is a different approach to this paper. Since their method is based on the information of further inland or deeper which is far from the seismogenic zone of the subduction, its sensitivity could be low especially for shallow areas near the trenches. On the other hand, our study is based on the information near the seismogenic zones, including the frontal portion of the wedge. Thus, we could determine the spatial heterogeneity along the trench which might dominate the focal area with high spatial resolution and discuss the correlation to the overshoot area. Our proposed method should be better designed for the discussion of such along-trench heterogeneity for the subduction earthquake.

The application of the above concept to the Japan Trench clearly indicated that the seafloor slope angle (relative μ_b') is systematically smaller within the area of the large coseismic shallow rupture during the 2011 earthquake than those of the southern and northern areas, where little coseismic slip was imaged. The correlation between the seafloor topography and the slip distribution should contribute the linkage between the seismology and tectonics.

Acknowledgments, Samples, and Data

Acknowledgments: Yamaguchi, A. advised fundamental research of frontal prism. We acknowledge two anonymous reviewers for their thoughtful reviews.

Data and materials availability: The bathymetry data used in the calcuration are obtained from Kishimoto, K. (2000). Our calculation results are available in https://doi.org/10.6084/m9.figshare.12546455.v2.

References

Bilek, S. L., & Lay, T. (2002). Tsunami earthquakes possibly widespread manifestations of frictional conditional stability. *Geophysical Research Letters*, *29*(14), 18-1-18–4. doi.org/10.1029/2002gl015215

Chester, F. M., Rowe, C., Ujiie, K., Kirkpatrick, J., Regalla, C., Remitti, F., Moore, J. C., Toy, V., Wolfson-Schwehr, M., Bose, S., Kameda, J., Mori, J. J., Brodsky, E. E., Eguchi, N., & Toczko, S. (2013). Structure and composition of the plate-boundary slip zone for the 2011 Tohoku-Oki earthquake. *Science*, *342*(6163), 1208–1211. doi.org/10.1126/science.1243719

Currie, C. A., Hyndman, R. D., Wang, K., & Kostoglodov, V. (2002). Thermal models of the Mexico subduction zone: Implications for the megathrust seismogenic zone. *Journal of Geophysical Research: Solid Earth*, *107*(B12), ETG 15-1-ETG 15-13. doi.org/10.1029/2001jb000886

Dahlen, F. (1990). Critical Taper Model Of Fold-And-Thrust Belts And Accretionary Wedges. *Annual Review of Earth and Planetary Sciences*, *18*(1), 55–99. doi.org/10.1146/annurev.earth.18.1.55

Dahlen, F. A. (1984). Noncohesive Critical Coulomb Wedges: an Exact Solution. *Journal of Geophysical Research*, *89*(B12), 10125–10133. doi.org/10.1029/JB089iB12p10125

Davis, D., Suppe, J., & Dahlen, F. A. (1983). Mechanics of fold-and- thrust belts and accretionary wedges. *Journal of Geophysical Research*, *88*(B2), 1153–1172. doi.org/10.1029/JB088iB02p01153

Dielforder, A., Hetzel, R., & Oncken, O. (2020). Megathrust shear force controls mountain height at convergent plate margins. *Nature*, *582*(June). doi.org/10.1038/s41586-020-2340-7

Fagereng, A. (2011). Wedge geometry, mechanical strength, and interseismic coupling of the Hikurangi subduction thrust, New Zealand. *Tectonophysics*, *507*(1–4), 26–30. doi.org/10.1016/j.tecto.2011.05.004

Fujiwara, T., Yamazaki, T., & Joshima, M. (2001). Bathymetry and magnetic anomalies in the Havre Trough and Southern Lau Basin: From rifting to spreading in back-arc basins. *Earth and Planetary Science Letters*, *185*(3–4), 253–264. https://doi.org/10.1016/S0012-821X(00)00378-2

Fulton, P. M., Brodsky, E. E., Kano, Y., Mori, J., Chester, F., Ishikawa, T., Harris, R. N., Lin, W., Eguchi, N., & Toczko, S. (2013). Low coseismic friction on the Tohoku-Oki fault determined from temperature measurements. *Science*, *342*(6163), 1214–1217. doi.org/10.1126/science.1243641

Hirano, N., Takahashi, E., Yamamoto, J., Abe, W., Ingle, S. P., Kaneoka, I., Hirata, T., Kimura, J. I., Ishii, T., Ogawa, Y., Machida, S., & Suyehiro, K. (2006). Volcanism in response to plate flexure. *Science*, *313*(5792), 1426–1428. doi.org/10.1126/science.1128235

Kimura, G., Hina, S., Hamada, Y., Kameda, J., Tsuji, T., Kinoshita, M., & Yamaguchi, A. (2012). Runaway slip to the trench due to rupture of highly pressurized megathrust beneath the middle trench slope: The tsunamigenesis of the 2011 Tohoku earthquake off the east coast of northern Japan. *Earth and Planetary Science Letters*, *339–340*, 32–45. doi.org/10.1016/j.epsl.2012.04.002

Kishimoto, K. (2000). Combined Bathymetric and Topographic Mesh Data: Japan 250m Grid. *Open File Rep. 353, 1-CD-ROM*.

Kodaira, S., No, T., Nakamura, Y., Fujiwara, T., Kaiho, Y., Miura, S., Takahashi, N., Kaneda, Y., & Taira, A. (2012). Coseismic fault rupture at the trench axis during the 2011 Tohoku-oki earthquake. *Nature Geoscience*, *5*(9), 646–650. doi.org/10.1038/ngeo1547

Koge, H., Hamahashi, M., Kimura, G., Fujiwara, T., Kodaira, S., Hamada, Y., Sasaki, T., Kameda, J., Kitamura, Y., Fukuchi, R., Yamaguchi, A., & Ashi, J. (2014). Friction properties of the plate boundary megathrust beneath the frontal wedge near the Japan Trench: An inference from topographic variation Multidisciplinary. *Earth, Planets and Space*, *66*(1), 1–10. doi.org/10.1186/s40623-014-0153-3

Lallemand, S. E., Schnürle, P., & Malavieille, J. (1994). Coulomb theory applied to accretionary and nonaccretionary wedges: Possible causes for tectonic erosion and/or frontal accretion. *Journal of Geophysical Research: Solid Earth*, *99*(B6), 12033–12055. doi.org/10.1029/94jb00124

Mochizuki, K., Yamada, T., Shinohara, M., Yamanaka, Y., & Kanazawa, T. (2008). Weak interplate coupling by seamounts and repeating M ~ 7 earthquakes. *Science*, *321*(5893), 1194–1197. doi.org/10.1126/science.1160250

Nishikawa, T., Matsuzawa, T., Ohta, K., Uchida, N., Nishimura, T., & Ide, S. (2019). The slow earthquake spectrum in the Japan Trench illuminated by the S-net seafloor observatories. *Science*, *365*(6455), 808–813. doi.org/10.1126/science.aax5618

Sun, T., Fujiwara, T., Kodaira, S., He, J., & Wang, K. (2017). Tohoku-oki earthquake. *Nature Communications*, *8*(May 2016), 1–8. doi.org/10.1038/ncomms14044

Tsuru, T., Park, J.-O., Miura, S., Kodaira, S., Kido, Y., & Hayashi, T. (2002). Along-arc structural variation of the plate boundary at the Japan Trench margin: Implication of interplate coupling. *Journal of Geophysical Research: Solid Earth*, *107*(B12), ESE 11-1-ESE 11-15. doi.org/10.1029/2001jb001664

Ujiie, K., Tanaka, H., Saito, T., Tsutsumi, A., Mori, J., & Toczko, S. (2013). Low Coseismic Shear Stress on the. *Science*, *342*(December), 1211–1214. doi.org/10.1126/science.1243485

Wang, K., Brown, L., & Hu, Y. (2019). *Stable Forearc Stressed by a Weak Megathrust : Mechanical and Geodynamic Implications of Stress Changes Caused by the M = 9 Tohoku - Oki Earthquake Journal of Geophysical Research : Solid Earth*. 6179–6194. doi.org/10.1029/2018JB017043

Wang, K., & Hu, Y. (2006). Accretionary prisms in subduction earthquake cycles: The theory of dynamic Coulomb wedge. *Journal of Geophysical Research: Solid Earth*, *111*(6), n/a-n/a. doi.org/10.1029/2005JB004094

Wang, K., Hu, Y., von Huene, R., & Kukowski, N. (2010). Interplate earthquakes as a driver of shallow subduction erosion. *Geology*, *38*(5), 431–434. doi.org/10.1130/G30597.1

Figure 1. Schematic illustration of the critical taper model. A: Cross section of the forearc wedge in the Japan Trench (modified from Kimura et al., 2012). The area surrounded by the blue broken lines is the frontal wedge. B: Diagram showing the self-similar growth of a bulldozer wedge.

Figure 2. A: Cross plots between the Hubbert-Rubey pore fluid pressure ratio λ and basal friction μ_b' for a wedge. All extensionally critical states form the left limb of the critical state curve and all compressively critical states form the right limb. The stable region is under the curve (white). The straight-line tangent to the critical state curve represents the constant λ. B: Mechanically critical value of the frontal wedges controlled by the fluid pressure ratio within the prism (λ) versus effective basal friction (μ_b') in the straight-line and broken-line diagrams. The straight and broken lines represent different states of β. All extensionally critical states form the left limb of the critical state curve and all compressively critical states form the right limb. The stable field coincides with the critical state curve. The red straight line that intersects the critical state curve ideal the assumed the pore fluid pressure ratio λ. C: Graph of μ_b' with α and β varied from 1° to 5° for the general subduction wedge.

Figure 3 Geometrical diagram for evaluation of angle that deviates from the direction of the maximum slope angle. A: Top view. B: Cross section of OM. C: Cross section of OL. D: Diagram of the ratio α_m/α deviating by θ.

Figure 4. Relation of the 2011 Tohoku-Oki earthquake coseismic slip area and the distribution of the trench landward slope α in the Japan Trench. In the left map, the yellow star is the epicenter of the Tohoku-Oki earthquake, the contours show the compiled coseismic slip, the red straight lines are the positions of the bathymetrical profiles used to obtain α, the red broken lines are the rejected lines where R <0.9. The right figure shows the distribution of α. The red region corresponds to the coseismic slip area in the left figure. The orange line indicates the peak of the α histogram.

Figure 1.

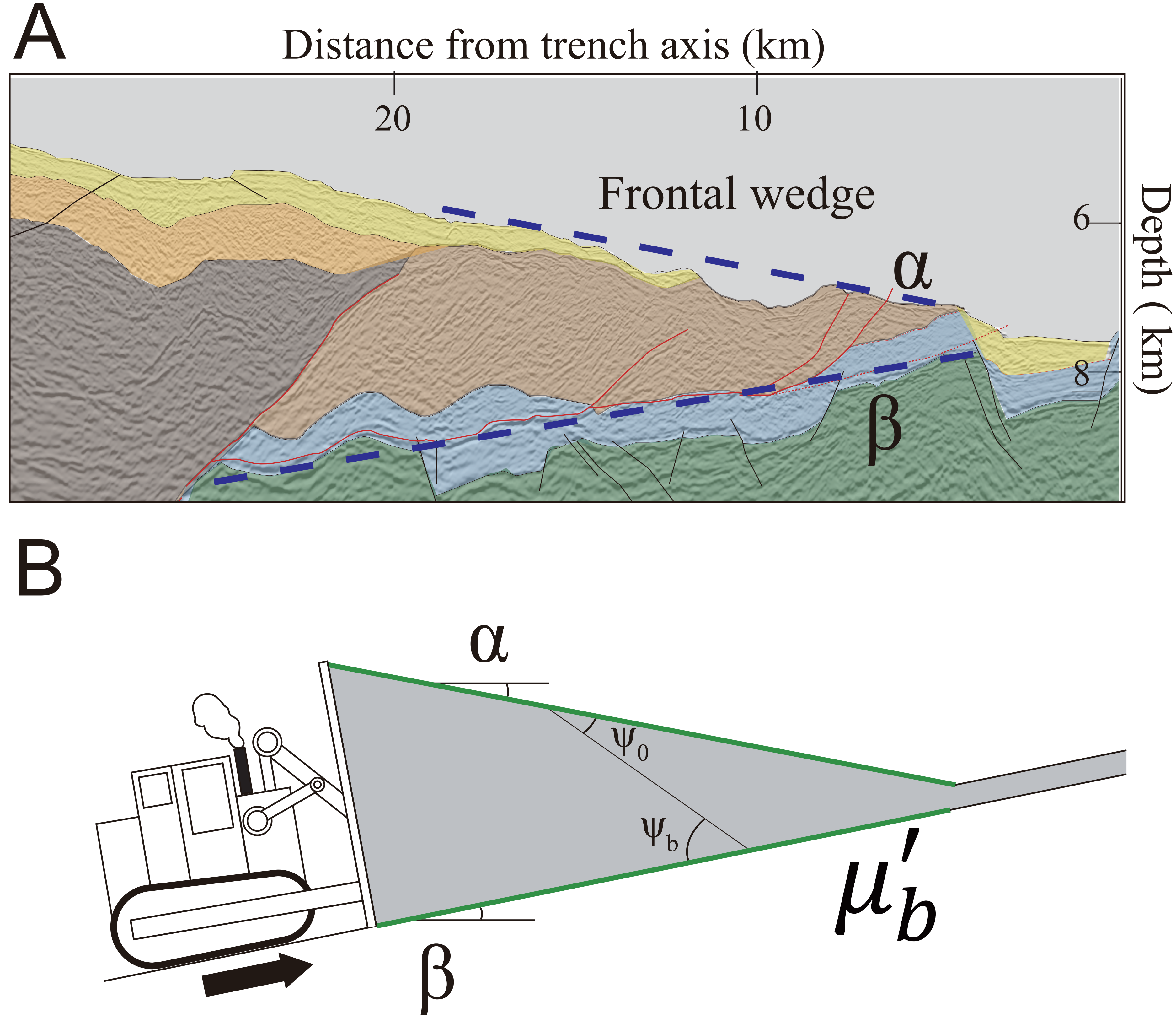
A
Distance from trench axis (km)
20
10
Frontal wedge
α
β
6
8
Depth (km)
B
α
ψ0
ψb
μ'b
β

Figure 2.

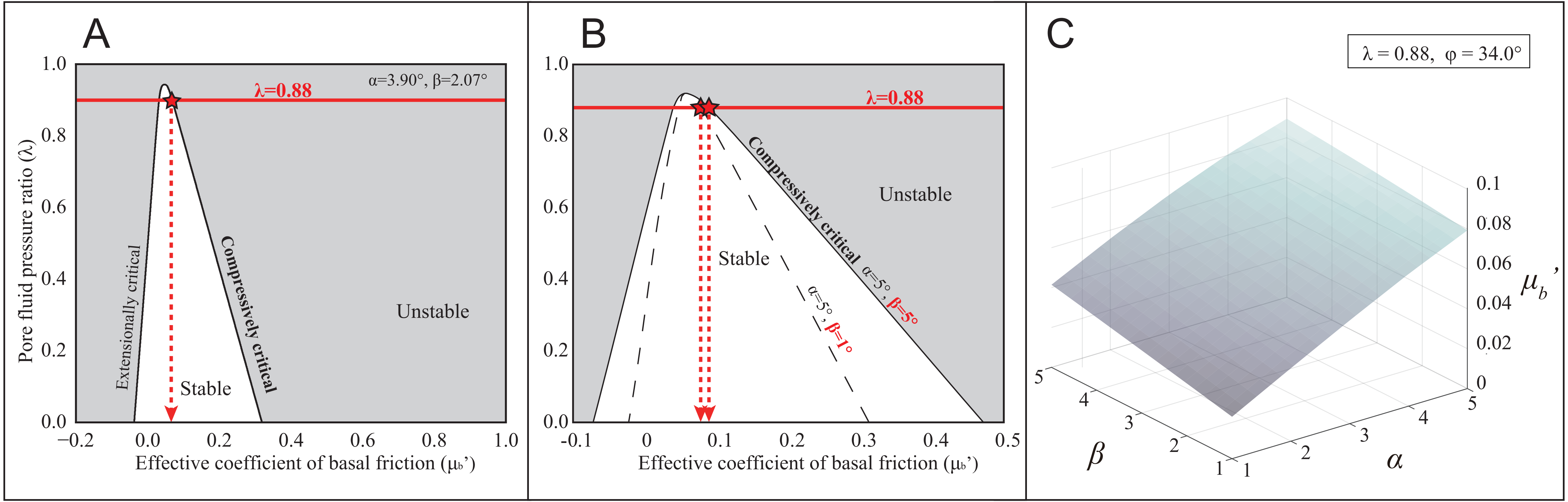

A
1.0
0.8
0.6
0.4
0.2
0.0
−0.2
0.0
0.2
0.4
0.6
0.8
1.0
Pore fluid pressure ratio (λ)
Effective coefficient of basal friction (μb')
λ=0.88
α=3.90°, β=2.07°
Extensionally critical
Compressively critical
Stable
Unstable
B
-0.1
0
0.1
0.2
0.3
0.4
0.5
Compressively critical
Unstable
Stable
α=5°, β=5°
α=5°, β=1°
C
λ = 0.88, φ = 34.0°
μb'
β
α
0.1
0.08
0.06
0.04
0.02
0
1
2
3
4
5

Figure 3.

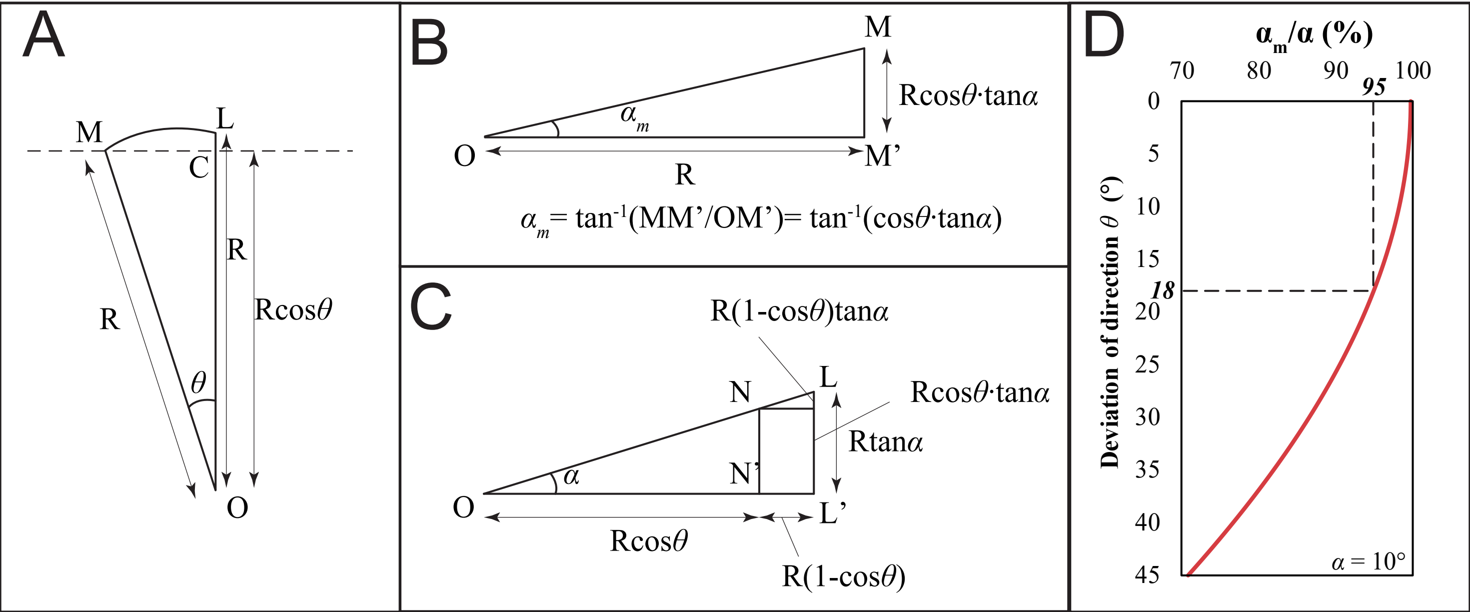
A
M
L
C
R
R
Rcosθ
θ
O
B
M
Rcosθ·tanα
α_m
O
M'
R
α_m = tan^-1(MM'/OM')= tan^-1(cosθ·tanα)
C
R(1-cosθ)tanα
L
N
Rcosθ·tanα
Rtanα
N'
α
O
L'
Rcosθ
R(1-cosθ)
D
α_m/α (%)
70
80
90
95
100
0
5
10
15
18
20
25
30
35
40
45
Deviation of direction θ (°)
α = 10°

Figure 4.

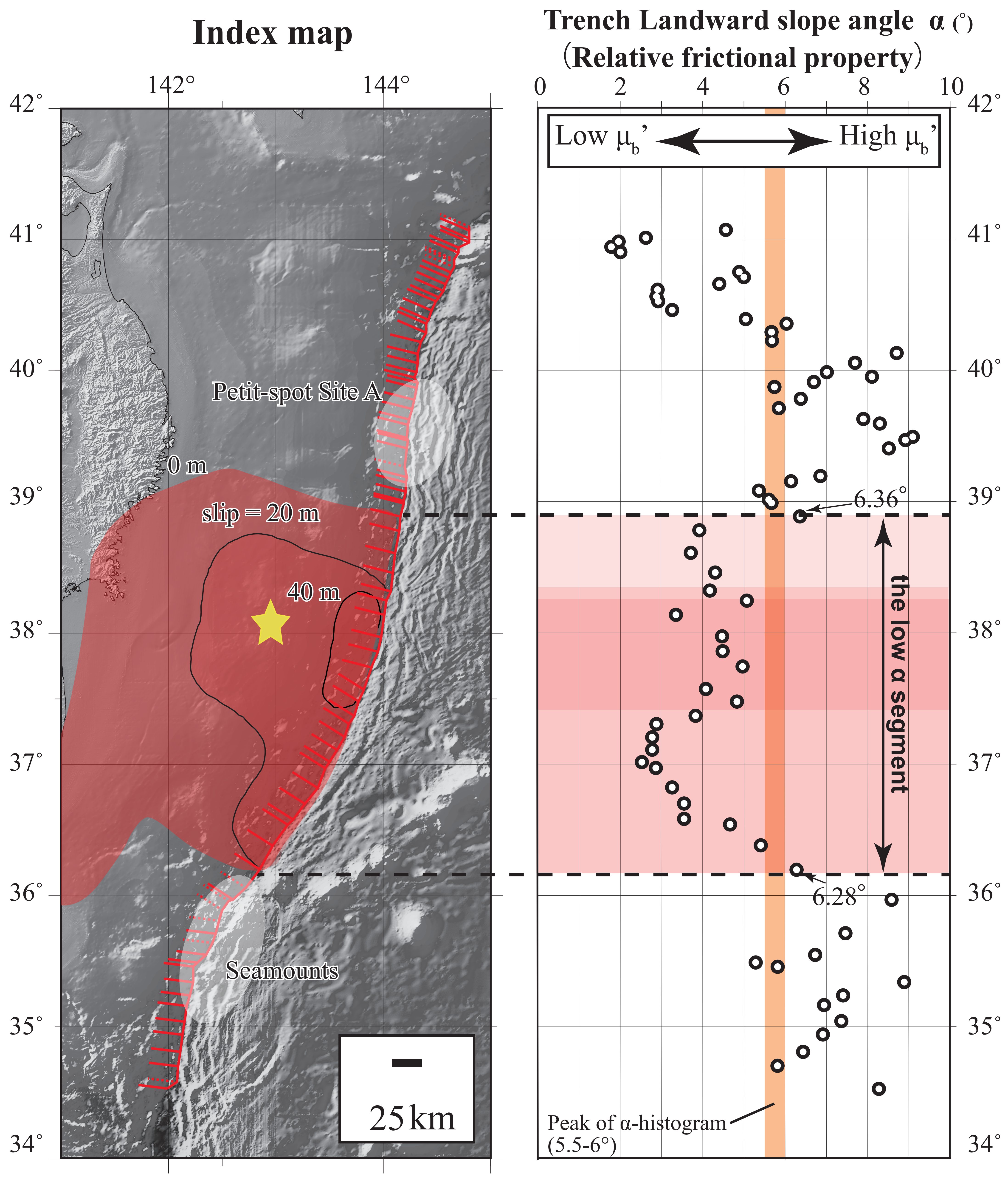

Index map
142°
144°
42°
41°
40°
39°
38°
37°
36°
35°
34°
Petit-spot Site A
0 m
slip = 20 m
40 m
Seamounts
25 km
Trench Landward slope angle α (°)
(Relative frictional property)
0
2
4
6
8
10
Low μb'
High μb'
6.36°
6.28°
the low α segment
Peak of α-histogram
(5.5-6°)